

Uranium-loaded apoferritin with antibodies attached: Molecular design for uranium neutron-capture therapy

(cancer/immunotherapy/apoferritin/chelation)

JAMES F. HAINFELD

Biology Department, Brookhaven National Laboratory, Upton, NY 11973

Communicated by Eugene P. Cronkite, August 11, 1992

ABSTRACT A method is described to deliver ^{235}U to tumors; the isotope would then be fissioned by incident neutrons, producing localized lethal radiation sufficient for therapy. Apoferritin was loaded with an average of ≈ 800 ^{238}U atoms per molecule. Stability of the loaded apoferritin in solution was improved, so that only 8% loss of uranium occurred after 8 days at pH 7. Fab' antibody fragments were covalently attached to the uranium-loaded apoferritin, and the immunoreactivity of the conjugate was 92% of that for antibody alone. Such bio-uranium constructions should provide significant advantages over boronated antibodies to meet the requirements for clinical neutron-capture therapy.

Neutron capture is a promising methodology for cancer therapy. Boron is the usual element used, but a system using uranium, as described here, may have significant advantages. Boron neutron-capture therapy is based upon localizing ^{10}B in a tumor and irradiation with slow neutrons (1). Upon neutron absorption, ^{10}B disintegrates to ^7Li and an α particle, and these ionizing particles can kill cells. Three approaches have been used in boron neutron-capture therapy: (i) use of boron compounds that localize in tumors (2); (ii) use of boron compounds that have specific metabolic uptake in tumor cells (3); and (iii) use of boron coupled to anti-tumor antibodies. Based upon antibody sites per tumor cell (10^5 – 10^6) and the concentration of boron necessary for therapy (>15 ppm), it has been estimated that ≈ 1000 boron atoms per antibody are required (4). This result has been difficult to achieve, and although recent progress has been made (5), no *in vivo* localization of the required amount of ^{10}B has been demonstrated. Studies have shown that solid carcinomas exhibit a heterogeneous pattern of antibody distribution (different amounts of antibodies on different cells), have variable vascularity that could limit antibody uptake (6), and show poor penetration of antibodies beyond a few cell layers (7). Because the α and Li particles have a range of only about one cell, delivery of boron may be insufficient to many tumor cells.

To circumvent some of the problems with boron, uranium may be used instead; this was proposed some 51 yr ago (8). ^{235}U has a neutron fission cross section that is 6.6 times lower than the ^{10}B neutron-capture cross section (Table 1). However, a slow neutron splits the nucleus to two heavy charged ions producing 200 MeV, which is 71.4 times greater than the ^{10}B breakup energy. The fission fragments of ^{235}U have a longer range, giving a volume advantage of ≈ 8.4 over ^{10}B . Another factor is the effectiveness of these particles in sterilizing cells. Although the ^{235}U fission fragments deposit an average of ≈ 28 times more energy per μm (measured in $\text{keV}/\mu\text{m}$ or linear energy transfer), their effectiveness is not greater by this factor because at some level a cell is killed;

further energy deposition is then of no value. Measurements using heavy-ion accelerators impinging on cells have yielded some data on the effectiveness of high linear energy transfer particles in killing cells (9). The average cell inactivation cross section for the ^{235}U fission products is ≈ 2.4 times greater than that for the ^{10}B fragments. The overall effectiveness of ^{235}U fission compared with ^{10}B breakup per atom for capture therapy may be estimated as a product of these factors (for the same neutron dose):

Advantage of ^{235}U to ^{10}B

$$= (\sigma_{fU}/\sigma_{n,\alpha B}) \times (V_U/V_B \times (\sigma_{\text{kill-U}}/\sigma_{\text{kill-B}})) \\ = (1/6.6) (8.4) (2.4) = 3.1,$$

where $\sigma_{fU}/\sigma_{n,\alpha B}$ is the neutron cross-section ratio (of ^{235}U fission to ^{10}B n, α production), V_U/V_B is the volume ratio (average volume of the two U fission products to the average volume of the two B breakup products), and $\sigma_{\text{kill-U}}/\sigma_{\text{kill-B}}$ is the ratio of the average cell-inactivation cross sections. The number of ^{235}U atoms required per antibody is then ≈ 320 (rather than 1000 for ^{10}B). This simplified estimate does not consider the other radiations emitted in ^{235}U fission (listed in Table 1), and more detailed calculations and experiments are needed to evaluate this potential advantage exactly. In any case, the ability of a ^{235}U fission to affect two cell layers rather than one for ^{10}B should be a significant advantage in most therapeutic strategies.

Only a few preliminary experiments on uranium neutron-capture therapy (UNCT) have been reported (10–12) (for review, see ref. 13), the most recent being 33 yr ago. None was pursued further, probably because of the toxicity of uranium compounds, their low uptake by common metal chelators, and the lack of methodology to attach hundreds of atoms per antibody.

This report focuses on the antibody-directed approach using ^{235}U for several reasons: (i) The longer range of the ^{235}U fission products compared to ^{10}B could provide effective radiation to a tumor, even though antibody distribution is nonuniform. (ii) Higher tumor-to-nontumor ratios are frequently obtained with antibody conjugates than with compounds alone. For example, a tumor-to-blood ratio of 11.9 was measured for an anti-carcinoembryonic antibody monoclonal antibody (14), whereas much lower ratios were observed for several small boron compounds (2, 3). (iii) Anti-human tumor antibodies are increasingly available to a wide range of tumors. (iv) Slowly growing and nondividing tumor cells are targeted (as well as dividing tumor cells) by antibodies; these may be missed by the metabolite-uptake method.

The approach to target a tumor immunologically with many uranium atoms attached to each antibody described here uses the protein ferritin. Ferritin (known to atomic resolution) has

Table 1. Comparison of ²³⁵U and ¹⁰B

	Neutron cross section, barns	Products	Energy, MeV	Range in water, μm	Linear energy transfer, keV/μm	Cell inactivation cross section, μm ²
²³⁵ U	583	⁸⁹ Kr, † ¹³⁶ Xe †	101.1 ‡ 63.9 ‡	18 11	5620 5810	38 100
¹⁰ B	3837	⁴ He (α), ³ Li	1.78 1.02	9 5	198 204	28 30
Ratio $\frac{U}{B}$						
Cross sections	1/6.6					
Average volumes	8.4					
Average cell inactivation cross sections	2.4					

Numbers in boldface type represent ratios as indicated.

*These data are from ref. 9.

†Kr and Xe are only examples (other fission products are possible).

‡ ²³⁵ U fission energy (MeV): Kinetic energy of fission fragments	165 ± 5
Prompt γ energy	7 ± 1
Kinetic energy of fission neutrons	5 ± 0.5
β particles from fission products	7 ± 1
γ rays from fission products	6 ± 1
Neutrinos from fission products	10
Total energy per fission	200 ± 6

a protein shell composed of 24 subunits with a central cavity in which up to 4500 iron atoms are carried as ferrihydrite (5 Fe₂O₃·9H₂O). Ferritin is 12.5 nm in diameter and contains an 8.0-nm central cavity that is empty in apoferritin (15). This central cavity volume should be adequate for the 320 uranium atoms required. Antibodies may be attached to the outer shell for tumor targeting (Fig. 1). By encapsulating the uranium within an autogenous protein, no immune response is expected, and heavy-metal toxicity should be minimized.

Accumulation of uranium in apoferritin has previously been seen. Harrison *et al.* (16) determined from x-ray data that UO₂²⁺ ions entered the central cavity region (through the hydrophilic channels) and that there were three specific binding sites per subunit within the central cavity. Electron microscopists, who commonly use uranyl acetate as a negative stain, have for many years shown images of apoferritin where uranium had leaked into the central cavities (17). This effect was reconfirmed more recently when intentional loading was an objective (18). Unfortunately, when prepared this way, essentially by air drying in a uranyl solution, apoferritin is damaged and not recoverable as intact uranium-loaded soluble molecules.

This report describes the achievement of three goals: stable loading of apoferritin with 800 or more uranium atoms, the

attachment of antibody to the loaded product, and demonstration of retention of immunoreactivity by this complex.

MATERIALS AND METHODS

Uranium Loading of Apoferritin. Method A included the following procedures: 1 mg of apoferritin (horse spleen, Sigma) was prepurified on a gel-filtration column (Superose 12, Pharmacia-LKB) to remove aggregates; eluent was 0.1 M ammonium acetate, pH 6.5. The sample was concentrated to 0.1 ml by using a Centricon-30 filter (Amicon) and then washed with 2 ml of water twice using the same filter. Then 0.3 ml of 0.2 M sodium phosphate buffer, pH 9, was added, and the mixture was incubated overnight. The sample was then applied to a gel-filtration column (GH25, Amicon) with 0.1 M Tris, pH 7.5, as the eluent. Time on the column was ≤6 min. To each 1-ml fraction tube, 1 ml of 1% or 0.1% uranyl acetate was added. After 1 hr, 1 ml of 0.2 M sodium phosphate buffer, pH 7.0, was added. After 30 min, the sample was filtered through a 0.1-μm filter and concentrated with a Centricon-30 filter. The concentrate was then applied to a gel-filtration column (Superose 12) running in 0.1 M Tris, pH 7.5. Method B was the same as method A, except that 2 ml of 0.03% uranyl acetate per 1-ml fraction was used. Method C was the same as method B, except that after initial isolation and concentration of the apoferritin, 0.3 ml of 0.1 M glycine-HCl, pH 4, was added (instead of pH 9 buffer).

Uranium and Protein Assay. Uranium loading alters the UV absorbance of apoferritin appreciably. Protein and uranium contents were estimated by measuring absorbances at 280 and 260 nm and calibrating their ratio by using direct measurements of uranium and protein. Protein concentrations were determined by the BCA method (Pierce). Five methods were used to determine uranium concentrations: (i) A chemical procedure using arsenazoIII (19); (ii) mass measurement of individual particles based on the elastic scattering of electrons in the scanning transmission electron microscope (STEM) (20); (iii) direct-current plasma emission spectrometry (Applied Research Labs, Valencia, CA); (iv) inductively coupled plasma mass spectrometry (ICPMS, VG Analytical, Manchester, U.K.); (v) neutron activation, where the ²³⁸U sample was irradiated by thermal neutrons, and γ decay of the ²³⁹Np produced was measured by using Compton suppression (21).

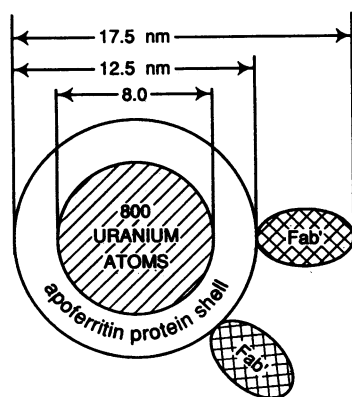


FIG. 1. Schematic drawing of apoferritin loaded with 800 uranium atoms in its central cavity. Fab' antibody fragments are covalently attached to the apoferritin protein shell to target the uranium to tumors.

Stability Testing. The solution stability of the uranium-loaded apoferritin was assayed by storing the purified product at 4°C in 0.1 M Tris buffer, pH 7, or goat serum (Sigma) and removing aliquots at various time intervals. These samples were passed over a gel-filtration column (Superose 12). Column fractions were analyzed for uranium and protein and examined by EM.

Fab' Antibody Attachment. Fab' antibody fragments were prepared from goat anti-mouse F(ab')₂ (Cappel) by adding 20 mM mercaptoethylamine/0.1 sodium phosphate, pH 7, for 1 hr and purifying the Fab' on a column (Superdex 75, Pharmacia LKB). Uranium-loaded apoferritin was pretreated with a 2000-fold molar excess of *N*-ethylmaleimide (dissolved in dimethyl sulfoxide) in 0.1 M sodium phosphate, pH 7/1 mM EDTA (20% dimethyl sulfoxide, final) for 1 hr to block reactive thiols, then purified on a column (GH25) in 0.1 M sodium phosphate, pH 7/1 mM EDTA. Sulfosuccinimidyl 4-(*N*-maleimidomethyl)cyclohexane-1-carboxylate (SMCC, Pierce) was dissolved in dioxane and added in nine equal amounts with agitation over 45 min at 30°C with a final 1000-fold molar excess over the apoferritin, and a final dioxane concentration of 8%. Incubation was continued for another 55 min at 30°C (22). The sample was applied to a column (GH25) to remove excess SMCC and mixed with an 8-fold molar excess of Fab' (to apoferritin). After incubation at 4°C for 16 hr, mercaptoethylamine was added (to a final concentration of 0.5 mM) for 2 hr to block unreacted crosslinker. The mixture was concentrated by using a Centricon-30 filter and purified on a column (Superose 12) with 0.1 M ammonium acetate buffer, pH 6.8.

Immunoreactivity. An antigen-affinity column was prepared by coupling mouse IgG (Sigma, 9.5 mg) to Affigel-10 (Bio-Rad, 3 ml) for 16 hr at room temperature with agitation. The gel was poured into a 1-ml column and prewashed with 10 ml of 10 mM Tris (pH 7.5), 10 ml of 0.1 M glycine (pH 2.5), 10 ml of 10 mM Tris (pH 8.8), 10 ml of 0.1 M triethylamine (pH 11.5), and then 20 ml of 10 mM Tris (pH 7.5). After a sample was loaded, flow was stopped for 1 hr to allow incubation with the gel. Eluting protein was reloaded and reincubated twice. The column was then cycled through the above washing protocol of buffers.

EM. Two microscopes were used, the Brookhaven STEM (20) to observe unstained samples and collect data for mass measurements and a Philips 300 microscope to view 2% uranyl acetate-stained samples.

RESULTS

Loading Mechanism. To achieve the high loading of apoferritin required for potential therapy (>300 uranium atoms per apoferritin), a strategy to actively concentrate uranium within the central cavity of apoferritin was developed. Soaking apoferritin in uranyl acetate solutions followed by air-drying produces infiltration of uranium into some molecules (17, 18). However, upon resolubilization, negligible amounts could be recovered as intact (loaded) apoferritin, even though a wide range of uranyl concentrations and extents of drying (including no drying) were tested. The loading observed by these procedures evidently occurs upon drying or if it does occur in solution, heavy aggregates are formed, so that single molecules are not recoverable by gel-filtration column chromatography. The method reported here that was successful relies upon a crystallization process where uranium crystals are nucleated and grown inside apoferritin. This method was achieved by controlling the solubility of the uranyl ion. Uranyl acetate is soluble at pH < ≈4.5, but conversion to insoluble uranyl complexes occurs at higher pHs. Because the apoferritin shell is stable at pH 4, soaking in a UO₂(OAc)₂ solution would be predicted to allow UO₂²⁺ to enter the central cavity; then raising the pH to ≈7 should form an

insoluble precipitate within the shell that may be stable at physiological pH 7.4. The result was as predicted. Because phosphate also forms an insoluble complex with UO₂²⁺ ions at pH 7, phosphate buffer was also used to crystallize the uranium. The insoluble uranium was most likely mixed salts of hydrated sodium uranyl phosphate and acetate; in the optimized procedure, the ratio of phosphate to acetate was 240, so acetate was a minor component. Although some bulk crystallization occurred throughout the solution, the apoferritin could be completely isolated because of its distinctive size. This isolation was done by first using a 0.1-μm filter to remove large crystals from the solution and then using gel filtration to separate out the protein. EM showed that most treated apoferritin molecules now had dense cores (Fig. 2).

Stability of Loaded Apoferritin. Solution stability was studied by passing an aliquot of the sample over a gel-filtration column at various times after preparation to separate the loaded apoferritin from any uranium that had escaped or from any apoferritin that had broken down. Conditions that produced loading with large amounts of uranyl acetate showed a substantial loss of uranium and intact apoferritin with time (Fig. 3). EM revealed that the product had some uranium encapsulated but that many crystals were larger than the apoferritin cavity and distorted the apoferritin shell. After several hours, much of the apoferritin had disintegrated into variously sized fragments (Fig. 4), the smallest being subunit-sized (20.7 ± 8.6 kDa, 111 particles measured by STEM mass analysis; apoferritin subunits are 18.8 kDa). Growing uranyl crystals within the apoferritin central cavity may have exerted too much mechanical force on the protein shell, causing it to fragment. The initial average loading was low (≈150), presumably because minimally ruptured apoferritins that had lost their uranium (Fig. 4) were not separated from loaded ones by the gel-filtration column used, giving a low average loading. Reducing the amount of uranyl acetate produced molecules with an average of ≈400 uranium atoms that were stable even after 8 days.

Maximal Loading of Apoferritin. A further objective was to maximally load the apoferritin. One important parameter was the initial pH of the apoferritin central cavity. Apoferritin preincubated in pH 9 buffer showed ≈400 uranium atoms per

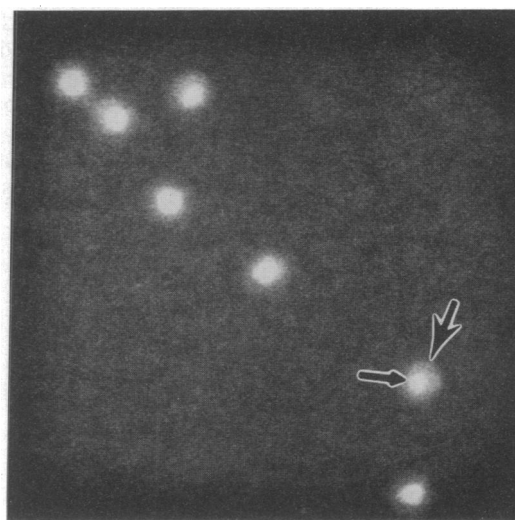


FIG. 2. STEM dark-field micrograph of apoferritin molecules loaded with ≈800 uranium atoms each (*Materials and Methods*, method C). The insoluble dense uranyl phosphate cores appear bright (small arrow) and are surrounded by the apoferritin protein shell (grey density, larger arrow) in this unstained sample. Note even filling of the central cavities without distention or overfilling and absence of breakdown products in background. (Full width of Fig. 2 is 128 nm.)

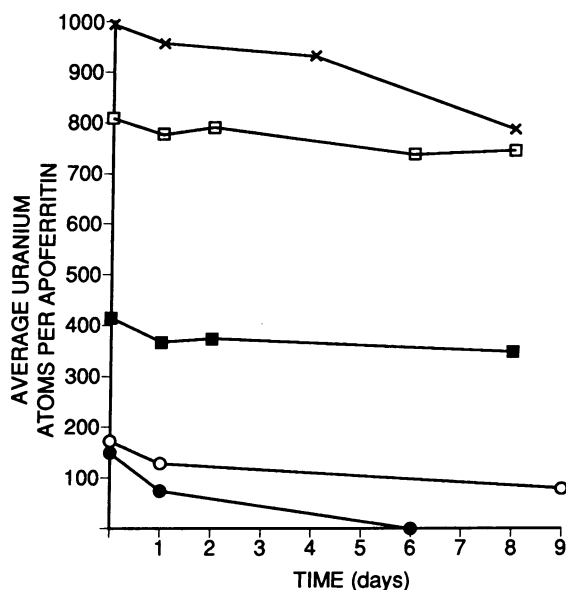


FIG. 3. Time stability of uranium-loaded apoferritin. Use of larger amounts of uranium in preparation (1% uranyl acetate) resulted in poor stability (●, *Materials and Methods*, method A). Reducing uranium to 0.1% improved stability (○, method A, 0.1%), and use of 0.03% further enhanced stability (■, method B). Use of pH 4 instead of pH 9 preincubation improved the loading (□, method C). Incubation of loaded apoferritin (by method C) incubated in serum rather than buffer is also shown (×).

central cavity, whereas preincubation in pH 4 buffer gave ≈ 800 atoms per central cavity (Fig. 2). The lower pH may have given UO_2^{2+} longer solubility in this dynamic process, allowing the ion to nucleate at more sites in the apoferritin shell, leading to more uniform filling (cf. Figs. 2 and 4, where spherical filling is seen with pH 4, but longer needles are seen with pH 9). The pH 4 preloaded samples showed 92% retention of uranium loading and virtually no loss of protein after 8 days (Fig. 3). Incubation in goat serum instead of buffer showed similar stability (Fig. 3).

Accumulation of uranium in the apoferritin central cavities by these procedures is an active process. Eight hundred uranium atoms accumulated within the apoferritin central

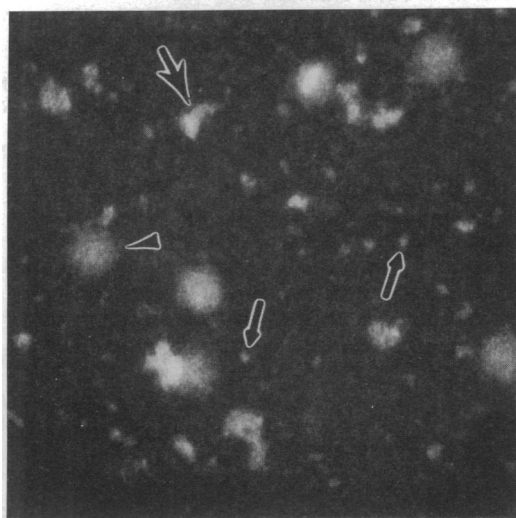


FIG. 4. Extensively broken down apoferritin caused by uranium overloading (method A, 1% uranyl acetate). Background is littered with globular proteins with the weight of apoferritin subunits (small arrows) as well as larger-shell fragments (larger arrow) and empty molecules (arrowhead). Sample was prepared several hours after column purification. (Full width of Fig. 4 is 128 nm.)

cavity volume corresponds to a 10^4 increase over a 0.02% uranyl acetate solution. This amount of loading would use up all of the available uranium in solution, leaving none for crystallization outside the apoferritin. This calculation suggests that there is specific nucleation within the apoferritin central cavities, probably at the uranyl ion-binding sites. A consequence of this almost quantitative uptake of solution uranium by apoferritin was demonstrated by using 2.5 times the amount of apoferritin, keeping all other conditions identical. The loading dropped from ≈ 800 to ≈ 400 uranium atoms per apoferritin molecule. Presumably all of the uranyl ions were depleted, and loading could not proceed further.

Quantitation of Loading. Chemical methods had low sensitivity and were only useful for large amounts of material. STEM mass measurement of single molecules gave a molecular mass of 704 ± 144 kDa (152 particles). This result translated into 633 ± 360 uranium atoms per molecule, assuming a core composition of $UO_2PO_4 \cdot 2H_2O$. The same sample measured by ICPMS gave 814 uranium atoms per apoferritin. Individual particles had as many as 2090 uranium atoms. Direct-current plasma emission spectrometry (0.04 ppm detection limit with the instrument used) gave values consistent with other measurements; a sample with uranium at 0.98 ppm by direct-current plasma emission spectrometry gave a value of 1.11 ppm by ICPMS. ICPMS, the most sensitive technique (0.05–0.1 parts per billion detection limit), gave 814 uranium atoms per apoferritin using the best loading procedure (*Materials and Methods*, method C). Neutron activation (≈ 1 –5 parts per billion detection limit) showed a moderately loaded sample to contain 144 uranium atoms per apoferritin, whereas ICPMS of this sample indicated 167 atoms. The slight disparity in values of samples measured by different techniques was probably due to variations in sample handling (e.g., nebulization or dilution) for the different instruments and possibly slight adsorption to the test tube walls because the same sample was often analyzed weeks apart due to instrument availability. Controls (native apoferritin and buffers) showed no uranium, and standards gave expected values. Protein concentrations were measured by using BCA (Pierce); addition of uranyl acetate up to 10 times the highest expected sample amount did not affect this determination.

Coupling Loaded Apoferritin to Fab' Antibody Fragments. The use of Fab' antibody fragments was chosen to limit the overall size of the conjugate for better penetration into tissues. Fab' is $5 \times 4 \times 3$ nm, so that one Fab' attached to an apoferritin would be 17.5×12.5 nm (Fig. 1), close to the size of an IgG molecule (15 nm). Coupling resulted in up to several Fab' fragments covalently attached to the apoferritin shell (Fig. 5). Immunoreactivity of the final conjugate was tested on an immunoaffinity column where 8% was found not to bind, and the rest was recovered upon elution with glycine-HCl, pH 2.5, and Tris pH 8.8 buffers. The immunoreactivity was therefore 92%. Neither apoferritin nor uranium-loaded apoferritin bound to the column, whereas the specific goat anti-mouse $F(ab')_2$ had 98% binding.

DISCUSSION

Studies in radioimmunotherapy have shown that immunoconjugates maximally accumulate on the tumor (in mice) at ≈ 20 hr (23). Because clearance from nontumor tissues generally is more rapid than from the tumor, better tumor-to-nontumor ratios may be achieved after longer times. For example, in one study (24), after 4 days the tumor level dropped to $\approx 80\%$ of its maximum; however, there was about a 3-fold improvement in tumor-to-nontumor ratios. With UNCT, it is possible to choose the optimal time to irradiate after injection, which from these cited studies may be after ≈ 4 days.

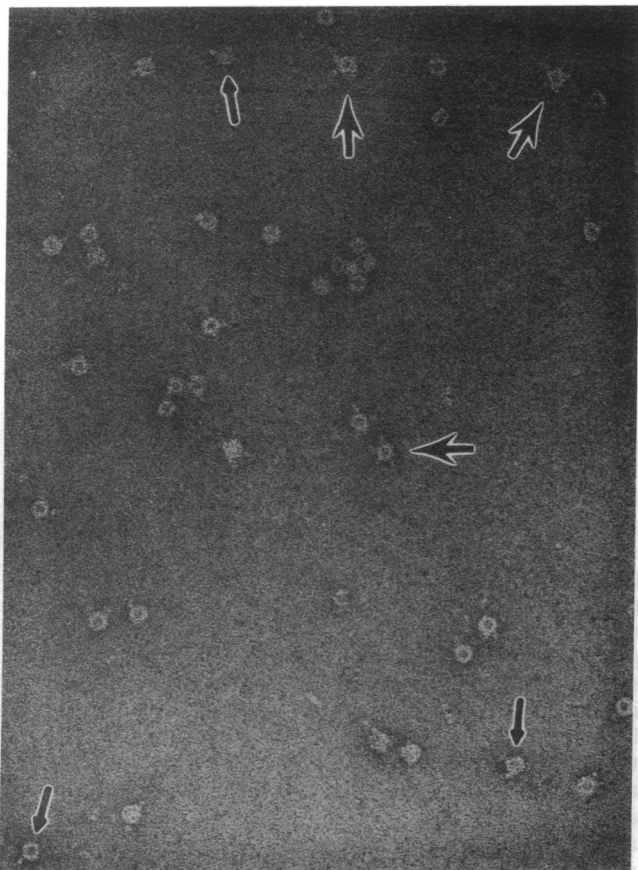


FIG. 5. Transmission electron micrograph of uranium-loaded apoferritin with a Fab' antibody fragment covalently attached (small arrows). Fab' fragments are the small nodules on the surface of the spherical apoferritin (cf. Fig. 1). Some molecules had multiple Fab' fragments attached (larger arrows) in this negatively stained sample. (Full width of Fig. 5 is 480 nm.)

Several attractive features of this uranium-delivery system for UNCT of tumors are as follows: (i) The uranium is encapsulated in a protein and should have much lower toxicity than do unencapsulated heavy-metal compounds. (ii) Because the uranium is "hidden" within a normal body protein (which could be cloned human apoferritin), no immunogenicity is anticipated, in contrast to potentially antigenic boron polymers. (iii) The number of Fab' fragments can be controlled per loaded apoferritin. Attachment of several Fab' fragments may be expected to increase the binding constant to antigens, possibly leading to better tumor targeting. (iv) The major shortcoming of radioimmunotherapy (now that stable chelates and immunoconjugates have been developed) is that the integrated dose to nontumor cells during antibody localization on the tumor is too high; insufficient dose to the tumor is generally delivered, being limited by the damage to other vital organs (25). In the approach proposed here, irradiation will occur in a short time window when tumor-to-nontumor localization is maximized. Also, the neutron beam will be confined to the tumor region, thus avoiding any damage to vital organs elsewhere. These advantages should be important in achieving effective therapy. Ferritin receptors exist on some normal cells (26) and could interfere with targeting. However, it should be possible to block these by preinjecting normal apoferritin before the uranium-loaded apoferritin is administered.

In addition to UNCT, this approach should be applicable to loading and delivering other useful compounds, elements, or radioisotopes to specific sites for diagnosis or therapy.

This uranium-biological chelate might also have materials science applications where the formation of small controlled size "nanocluster" particles is significant. For x-ray and electron energy-loss spectroscopy, this immunoprobe provides a distinctive signal (from the uranium). By using normal ferritin (loaded with iron) and apoferritin loaded with other materials, a group of differently "colored" probes could be developed for multiple label experiments.

In summary, a uranium-delivery system has been designed that appears to overcome some of the previous roadblocks to antibody-mediated neutron-capture therapy. The methods developed may also be of use in other diverse fields, such as immunochemistry, EM, and materials science.

The author thanks K. M. Carbone for excellent technical assistance as well as N. I. Feng, M. N. Simon, B. Y. Lin, and S. A. Landon. D. N. Slatkin and F. A. Dilmanian encouraged work on UNCT and assisted in calculations; J. S. Wall contributed helpful comments. ICPMS was done by M. S. Lin, and neutron-activation analysis was done by S. Landsberger. This work was supported by the Office of Health and Energy Research of the U.S. Department of Energy.

- Locher, G. L. (1936) *Am. J. Roentgenol.* **36**, 1-13.
- Joel, D. D., Fairchild, R. G., Laissue, J. A., Saraf, S. K., Kalef-Ezra, J. A. & Slatkin, D. N. (1990) *Proc. Natl. Acad. Sci. USA* **87**, 9808-9812.
- Coderre, J. A., Glass, J. D., Fairchild, R. G., Micca, P. L., Fand, I. & Joel, D. D. (1990) *Cancer Res.* **50**, 138-141.
- Fairchild, R. G. & Bond, V. P. (1985) *Int. J. Radiat. Oncol. Biol. Phys.* **11**, 831-840.
- Barth, R. F., Soloway, A. H., Adams, D. M. & Alam, F. (1992) in *Progress in Neutron Capture Therapy for Cancer*, eds. Allen, B. J., Moore, D. E. & Harrington, B. V. (Plenum, New York), pp. 265-268.
- Del Vecchio, S., Reynolds, J. C., Carrasquillo, J. A., Blasberg, R. G., Newmann, R. D., Lotze, M. T., Bryant, G. J., Farkas, R. J. & Larson, S. M. (1989) *Cancer Res.* **49**, 2783-2789.
- Langmuir, V. K., McGann, J. K., Buchegger, F. & Sutherland, R. M. (1991) *Nucleic Med. Biol.* **18**, 753-764.
- Zahl, P. A. & Cooper, F. S. (1941) *Radiobiology* **37**, 673-682.
- Wulf, H., Kraft-Weyrather, W., Miltenburger, H. G., Blakely, E. A., Tobias, C. A. & Kraft, G. (1985) *Radiat. Res.* **104**, S-122-S-134.
- McClintock, L. A. & Friedman, M. M. (1945) *Am. J. Roentgenol.* **54**, 704-706.
- Tobias, C. A., Weymouth, P. P., Wasserman, L. R. & Stapleton, G. E. (1948) *Science* **107**, 115-118.
- Knock, F. E. (1959) *Surg. Gynecol. Obstet.* **109**, 445-449.
- Slatkin, D. N. (1991) *Brain* **114**, 1609-1629.
- Philben, V. J., Jakowatz, J. G., Beatty, B. G., Vlahos, W. G., Paxton, R. J., Williams, L. E., Shively, J. E. & Beatty, J. D. (1986) *Cancer* **57**, 571-576.
- Ford, G. C., Harrison, P. M., Rice, D. W., Smith, J. M. A., Treffy, A., White, J. L. & Yariv, J. (1984) *Philos. Trans. R. Soc. London B* **304**, 551-565.
- Harrison, P. M., Andrews, S. C., Ford, G. C., Smith, J. M. A., Treffy, A. & White, J. L. (1987) in *Iron Transport in Microbes, Plants and Animals*, eds. Winkelmann, G., van der Helm, D. & Neilands, J. B. (VCH, Weinheim, Germany), pp. 445-475.
- Harris, J. R. (1982) *Micron* **13**, 169-184.
- Meldrum, F. C., Wade, V. J., Nimmo, D. L., Heywood, B. R. & Mann, S. (1991) *Nature (London)* **349**, 684-687.
- Marczenko, Z. (1976) in *Spectrophotometric Determination of the Elements* (Ellis Horwood, Chichester, U.K.), pp. 574-583.
- Wall, J. S. & Hainfeld, J. F. (1986) *Annu. Rev. Biophys. Biophys. Chem.* **15**, 355-376.
- Landsberger, S., Swift, G. & Neuhoff, J. (1990) in *Biological Trace Element Research*, ed. Schrauzer, G. N. (Humana, Clifton, NJ), pp. 27-32.
- Mahan, D. E., Morrison, L., Watson, L. & Haugneland, L. S. (1987) *Anal. Biochem.* **162**, 163-170.
- Andrew, S. M., Johnstone, R. W., Russell, S. M., McKenzie, I. F. C. & Pietersz, G. A. (1990) *Cancer Res.* **50**, 4423-4428.
- Smith, A., Groscurth, P., Waibel, R., Westera, G. & Stahel, R. A. (1990) *Cancer Res. (Suppl.)* **50**, 980s-984s.
- Yorke, E. D., Beaumier, P. L., Wessels, B. W., Fritzberg, A. R. & Morgan, A. C., Jr. (1991) *Nucleic Med. Biol.* **18**, 827-835.
- Moss, D., Powell, L. W., Arosio, P. & Halliday, J. W. (1992) *J. Lab. Clin. Med.* **119**, 273-279.